Bioorganic Chemistry 93 (2019) 103324

Contents lists available at ScienceDirect

Bioorganic Chemistry

journal homepage: www.elsevier.com/locate/bioorg

Design, synthesis and preliminary *in-vitro* studies of novel boronated monocarbonyl analogues of Curcumin (BMAC) for antitumor and β-amiloyd disaggregation activity

Emanuele Azzi[a,1], Diego Alberti[b,1], Stefano Parisotto[a], Alberto Oppedisano[a], Nicoletta Protti[c,d], Saverio Altieri[c,d], Simonetta Geninatti-Crich[b], Annamaria Deagostino[a,*]

[a] Department of Chemistry, University of Turin, via P. Giuria 7, 10125 Turin, Italy
[b] Department of Molecular Biotechnology and Health Sciences, University of Turin, via Nizza 52, 10126 Turin, Italy
[c] Department of Physics, University of Pavia, via Agostino Bassi 6, Pavia 27100, Italy
[d] Nuclear Physics National Institute (INFN), Unit of Pavia, via Agostino Bassi 6, Pavia 27100, Italy

ARTICLE INFO

Keywords:
Curcumin
MAC (Monocarbonyl analogues)
BMAC (Boronated Monocarbonyl Analogues)
Adenocarcinoma
Alzheimer's disease

ABSTRACT

Curcumin is currently being investigated for its capacity to treat many types of cancer and to prevent the neuron damage that is observed in Alzheimer's disease (AD). However, its clinical use is limited by its low stability and solubility in aqueous solutions. In this study, we propose a completely new class of boronated monocarbonyl analogues of Curcumin (BMAC, **6a-c**), in which a carbonyl group replaces the Curcumin β-diketone functionality, and an *ortho*-carborane, an icosahedral boron cluster, substitutes one of the two phenolic rings. BMAC antitumor activity against MCF7 and OVCAR-3 cell lines was assessed *in vitro* and compared to that of Curcumin and the corresponding MAC derivative. BMAC **6a-c** showed efficiencies that are comparable to that of MAC and superior to that of Curcumin in both the cell lines. Moreover, the inhibition of the formation of β-amyloid aggregates by BMAC **6a-c** was evaluated and it was shown that compound **6c**, which contains two OH moieties, has a better efficiency than Curcumin. The presence of a second –OH group can enhance the compound's binding efficacy with β-amyloid aggregates. For the future, the presence of at least one carborane group means that the BMAC antitumor effect can be coupled with Boron Neutron Capture Therapy.

1. Introduction

Curcumin [1], a naturally occurring molecule from *Curcuma longa*, has been found to have important therapeutic properties and has been widely investigated for use in a variety of treatment roles [2]. In fact, Curcumin has been proposed for use in cancer treatment and prevention, on the basis of a wide range of action mechanisms [3,4], and as a therapeutic agent for Alzheimer's disease (AD) [5–7], due to its ability to bind the amyloid β-peptide and modify its self-assembly pathway [8,9].

Some doubts about Curcumin's effectiveness have recently been raised, and these are mainly associated to its instability, which may affect its metabolic properties [10]. The reactivity of the β-diketone moiety (**A**, see Fig. 1) is one of the causes of this drawback. Indeed, the β-diketone moiety has been reported to be responsible for Curcumin instability at pH > 6.4 [11], and is the substrate of aldo-keto reductases, which can trigger the quick degradation of the molecule [12,13]. A great deal of effort has therefore been devoted to the synthesis of Curcumin analogues that can improve molecular stability [14–16]. Some remarkable examples of this can be found in chalcones (**B**, Fig. 1) [17,18], 1,3-diphenyl-2-propen-1-ones, which are one of the most important classes of flavonoids in the vegetal kingdom and which have shown promising pharmaceutical properties [17–20], and mono carboranyl analogues of Curcumin (MAC), in which a carbonyl group replaces the β-diketone functionality (**C**, Fig. 1) [21]. MAC have attracted considerable attention because they feature greater stability than Curcumin, thus retaining or even increasing biological activity, while also improving pharmacokinetics.

* Corresponding authors at: Department of Chemistry, University of Turin, via P. Giuria 7, 10125 Turin, Italy. (A. Deagostino). Department of Molecular Biotechnology and Health Sciences, University of Turin, via Nizza 52, 10126 Turin, Italy. (S.G. Crich).
E-mail addresses: simonetta.geninatti@unito.it (S. Geninatti-Crich), annamaria.deagostino@unito.it (A. Deagostino).
URL: http://orsy.unito.it (A. Deagostino).
[1] These authors contributed equally to this work

https://doi.org/10.1016/j.bioorg.2019.103324
Received 12 August 2019; Received in revised form 23 September 2019; Accepted 26 September 2019
Available online 27 September 2019
0045-2068/

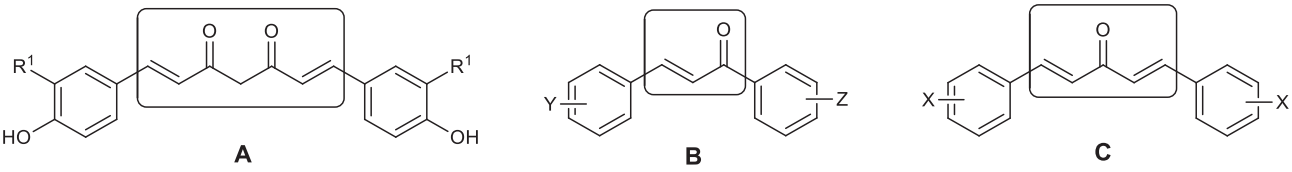

Fig. 1. Curcumin and Curcumin analogues. A: Curcumin, B: chalcones, C: Curcumin analogues in which a carbonyl moiety replaces a β–diketone functionality (MAC).

Interesting results have been reported in particular for MAC anti-inflammatory [22], and anticancer activity [23–26], (e.g., anti-prostate [27,28], -breast [29], -gastric [24,30], and -non-small-cell lung cancer [31–33]). A cell-apoptosis mechanism that is induced by endoplasmic reticulum stress has been hypothesised to explain these latter properties. This phenomenon would involve a reduced number of tumour cells than would be the case with Curcumin, thus suggesting that a different, more selective and peculiar, molecular mechanism is involved. This would also seem to indicate that there is a more specific and restricted range of targets for the antitumour activity of the mono-carbonyl analogues [23,34,35].

One innovative strategy that can be used to improve the pharmacological properties of biologically active substances is to introduce non-endogenous elements, such as boron, into their molecular structure [36]. In this context, carboranes, which are icosahedral boron clusters ($C_2B_{10}H_{12}$), have been proposed for use as the inorganic analogues of aromatic moieties in known drugs, thanks to their shape, hydrophobicity and *in-vivo* stability [37–40]. There have been reports of many examples of carborane-containing ligands that can target a number of different receptors/proteins (i.e., estrogen, androgen, PSMA, retinoic acid, HIV protease or enzyme inhibitors and, in the case of metallacarboranes, DNA) [41–45]. Moreover, boron compounds have been exploited, since 1930, in Boron Neutron Capture Therapy (BNCT) [46,47], which is a form of two-step radiotherapy that involves the targeted accumulation of non-radioactive ^{10}B in tumour cells, and their subsequent irradiation with epithermal neutrons. The captured neutrons generate two high-LET, short-range particles (α particles and lithium ions), which cause non-reparable damage to DNA. Moreover, the two high-energy particles release all their energy into a region that is comparable in size to a cell's diameter, thus locally limiting their effects. When the boron carriers selectively internalize ^{10}B at the pathological site, the neutron irradiation delivers a therapeutic dose without affecting the surrounding healthy tissues. This selectivity depends on the bio-distribution of the ^{10}B-containing compounds, and hence the technique can also be effective against disseminated metastases [48,49], and for isolated pathological zones surrounded by normal tissues. BNCT has been proposed as a treatment for various different pathologies, but most research focuses on cancer [50–52], and, in particular, the treatment of brain tumours. We have been carrying out pre-clinical studies on coupled BNCT-anticancer agents and MRI contrast agents in order to obtain an *in-vivo* quantification of boron distribution [53–59].

We herein propose the synthesis of new boronated monocarbonyl analogues of Curcumin (BMAC), which were obtained by substituting one benzene ring with an *ortho*-carborane cage, therapeutic properties, bioavailability and stability of Curcumin. It has recently been reported that the benzene ring is not the only aromatic ring that can guarantee bioactivity, but that it can be substituted with a furan, a thiophene, a pyrrole or naphtalin, which also exhibit inhibitory activity against a range of tumour cells [27,60]. It was shown that the substitution of benzene by other aromatic rings can maintain and even enhance the cytotoxic activities of mono-carbonyl analogues of Curcumin. To our knowledge, this is the first time that the aryl group has been substituted with a carborane moiety in MAC derivatives. Moreover, the presence of the carborane cage allows the synergistic merging of Curcuminoid therapeutic properties and neutron capture therapy to be performed in order to improve the use of these new derivatives (BMAC) as anticancer agents. Furthermore, the potential use of BMAC as inhibitors for β amyloid plaque formation has also been tested.

2. Results and discussion

2.1. Chemistry

In this work, we have tackled the task of preparing molecules that combine Curcumin structural properties and the carborane moiety. First, we had to consider the compulsory presence of a phenolic OH, which is necessary for both antitumor activity [61], and the inhibition of plaque formation [62]. Moreover, the different reactivity that carboranes show relative to an aryl group was a crucial item to be considered in the design of the synthetic strategy. Since monocarbonyl analogues of Curcumin MAC (B, Fig. 1) have been demonstrated to possess Curcumin-like activity and a higher stability than dicarbonyl derivatives, we conceived a BMAC derivative that contains both a carborane unit and a substituted phenol, linked by a conjugated dienoyl moiety (structure 6, Scheme 1). This linkage should fit the structural properties reported by Reinke and co, who fixed the ideal length between the active units at 16 Å in order to favour efficacy in plaque disaggregation.[63] With this goal in mind, we designed a synthetic strategy in which a formyl carborane **1** is coupled to hydroxyphenylprop-3-en-2-one (**4**) via an aldol reaction. Enone **4** can be prepared via the condensation of acetone **3** with the suitably substituted hydrobenzaldehyde **2**, as seen in Scheme 1.

We performed the selective mono-deprotonation of an *ortho*-carborane with *n*-BuLi, in high dilution conditions, and the subsequent reaction with a suitable electrophile, following the procedure reported by Dozzo et al. [64], in which an excess of methyl formate was added to the intermediate carboranyl anion.

At this stage, we turned our attention to the preparation of phenol-containing moiety **4**, which was carried out via aldol condensation with acetone. The latter, which bears two acidic sites, undergoes two subsequent condensations with an aromatic aldehyde (**2a-c**) and the formylcarborane **1** allowing the "hybrid" carbo-Curcumins **6** to be obtained. In order to evaluate the influence of the methoxyl and hydroxyl substituents on the aromatic ring, three substrates were considered, namely vanillin (**2a**), 4-hydroxybenzaldehyde (**2b**) and 3,4-dihydroxybenzaldehyde (**2c**), whose phenolic functionalities were all protected with a THP (tetrahydropyranyl) group before aldol condensation, in consideration of their acidity, as seen in Scheme 2.

The condensation that resulted in 4-(4-tetrahydropyranyloxyaryl)-but-3-en-2-ones **4a, 4b** and **4c** was accomplished with an excess of NaOH and using acetone as both reagent and solvent. The products were recovered in good yields (85, 90 and 86% for **5a, 5b** and **5c** respectively), as seen in Scheme 2.[65]

Subsequently, a second aldol condensation between formylcarborane **1** and chalcones **4** was carried out to obtain aldols **5**. The implemented synthetic procedure relies on: (*i*) the fact that carborane cages are degraded to *nido* carboranes via treatment with nucleophilic bases; and (*ii*) the reactivity of aldehyde **1** is more similar to that of a much less reactive aliphatic than that of an aromatic derivative. At first, we carried out the reaction under the conditions reported by Mahrwald et al., who used catalytic amounts of Et_3N in the

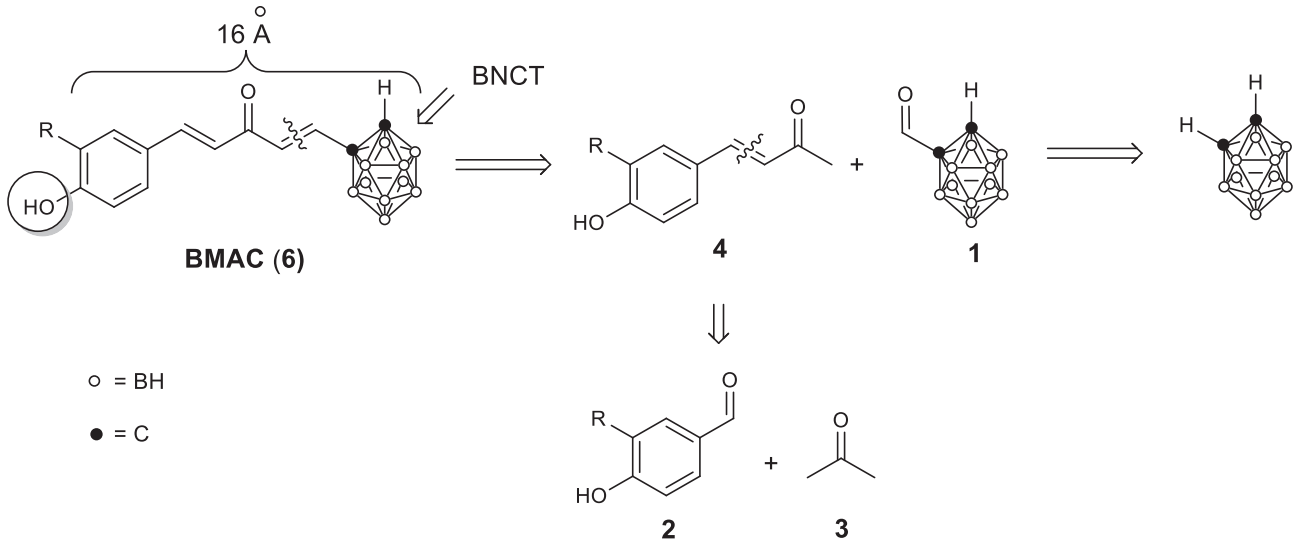

Scheme 1. Retrosynthetic scheme for the synthesis of BMAC.

presence of $LiClO_4$ for the aldol condensation of benzaldehyde and either ketones or alcohols, both primary and secondary [66], which was then extended to aliphatic aldehydes [67]. Unfortunately, all attempts to apply this procedure to formylcarborane **1** and chalcone **4b** were unsuccessful. We thus decided to use LDA (lithium diisopropylamide), whose nucleophilicity is negligible, for the formation of the enolate of 4-(4-tetrahydropyranyloxymethoxyphenyl)-but-3-en-2-one **4b**. This latter, formed *in situ* after three hours, was reacted with aldehyde **1** in THF and the corresponding carboranyl aldol derivative was recovered in a 54% yield. The reaction was then extended to **4a** and **4c**, affording the desired products **5a** and **5c** in similar yields (55 and 57%, respectively), see Scheme 2. Aldol formation was supported by NMR spectra, in which the signals pertinent to CH and CH_2 were detected in both ^1H and ^{13}C NMR. Compounds **5a**, **5b** and **5c** were then treated with a solution of H_2SO_4 (10% w/w in water) in refluxing THF, giving 1-*o*-carboranyl-5-(4-hydroxyoaryl)-penta-1,5-dien-3-ones (**6a**, **6b**, **6c**) in good yields. This procedure allowed the simultaneous deprotection of THP and the formation of the second conjugated double bond to occur via an elimination reaction. The structure of the products was elucidated by NMR. The ^1H NMR spectra show a broad singlet, which is pertinent to the CH of the *o*-carborane, at 4.96 ppm for all three derivatives, **6a**, **6b** and **6c**, demonstrating the presence of the carborane cage. Moreover, two AB systems were easily detected for the protons of the double bonds. Two doublets were present, at 7.63 and 6.89 ppm, and these can be accounted for by the protons associated with the double bond that is conjugated with the aromatic ring, while the two at 7.09 and 6.97 ppm, for those linked to the carborane. Moreover, the stereoselective formation of the (1*E*,4*E*)-1-aryl-5-carboranylpenta-1,4-dien-3-ones **6a**, **6b** and **6c** was confirmed by the large value of the coupling constants (16.0 and 15.4 Hz respectively).

In order to carry out the evaluation of the biological activity of BMAC **6a**, **6b** and **6c**, the monocarbonyl analogues of Curcumin, (1*E*,4*E*)-1,5-bis(4-hydroxy-3-methoxyphenyl)-penta-1,4-dien-3-one (**7**, Fig. 2) and (1*E*,4*E*)-1,5-bis(*C-ortho*-carboranyl)-penta-1,4-dien-3-one (**8**, Fig. 2) were synthesised.

Both derivatives were prepared via an aldol condensation. (1*E*,4*E*)-1,5-bis(4-hydroxy-3-methoxyphenyl)- penta-1,4-dien-3-one (**7**) was prepared in good yields. The low reactivity of formyl carborane **1**, which is similar to that of aliphatic aldehydes, made the preparation of *bis* carboranyl pentenone **8** much more difficult, and only the previously reported procedure, which utilizes catalytic Et_3N with $LiClO_4$, was found to be effective. (1*E*,4*E*)-1,5-Bis(*C-ortho*-carboranyl)-penta-1,4-dien-3-one (**8**), acetone **3** and formylcarborane **1** were reacted for five days in refluxing toluene, producing **8** in a 21% yield. The proper structure was fully consistent with the NMR spectra.

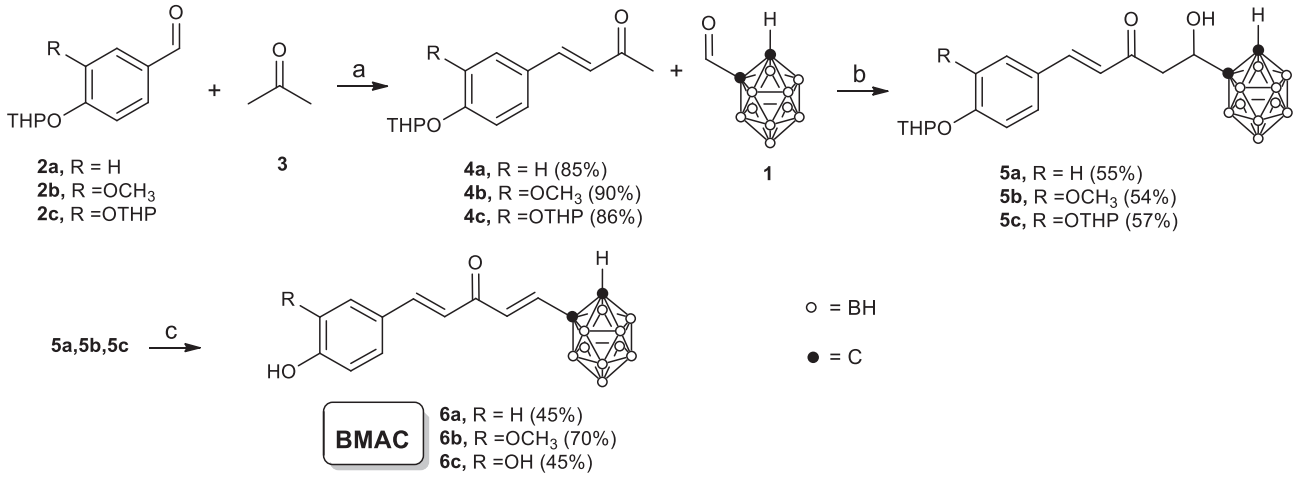

Scheme 2. Synthesis of substituted 1-*o*-carboranyl-5-(4-hydroxyohexyl)-penta-1,5-dien-3-ones (6a, 6b, 6c). Reaction conditions: (a) NaOH (1.5 eq.), acetone, 0 °C then rt; (b) LDA (1.1 eq.), THF, −78 °C then 1 (1 eq.), −78 °C; then H_2O, 0 °C then rt (c) H_2SO_4 (10% in water), THF, reflux.

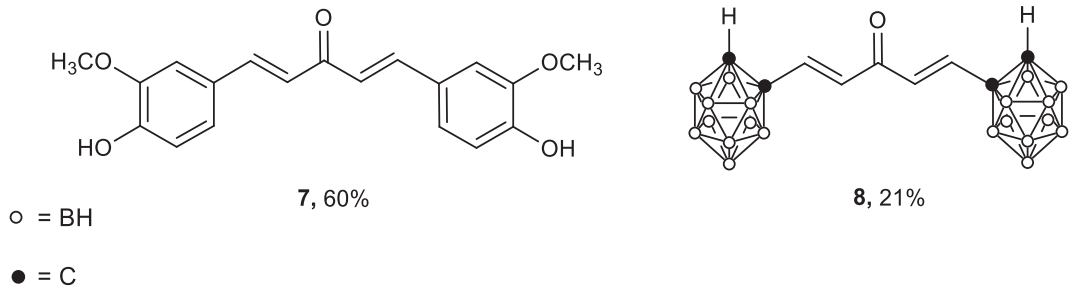

Fig. 2. Structures of (1*E*,4*E*)-1,5-bis(4-hydroxy-3-methoxyphenyl)-penta-1,4-dien-3-one 7 and (1*E*,4*E*)-1,5-bis(*C-ortho*-carboranyl)-penta-1,4-dien-3-one **8**.

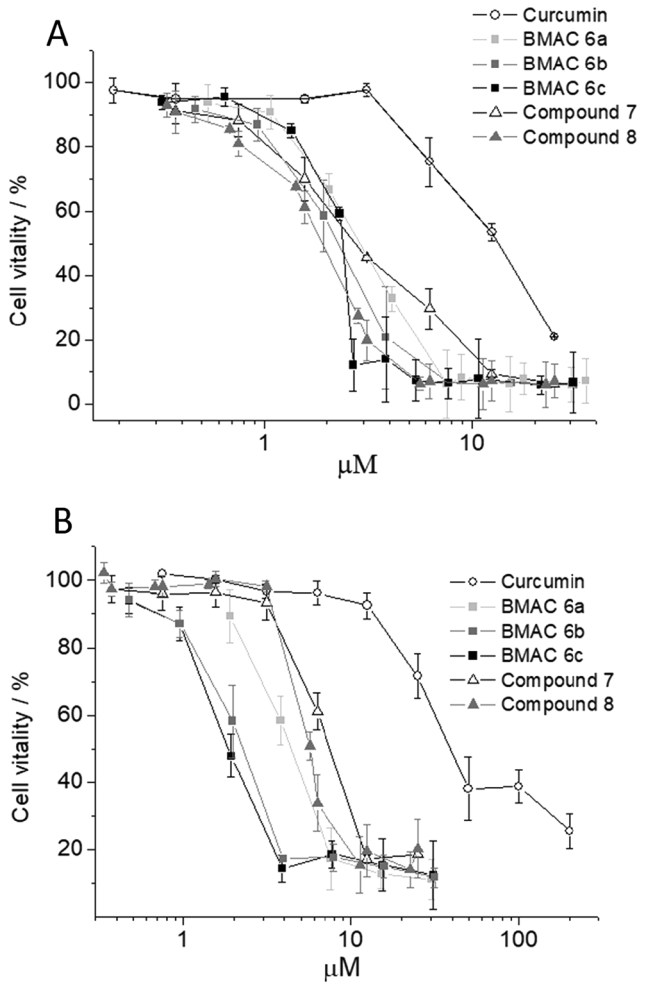

Fig. 3. MCF7 (3A) and OVCAR-3 (3B) cell vitality measured in the MTT assay as a function of the concentration of Curcumin and the mono-carbonyl compounds (**6a**, **6b**, **6c**, **7**, **8**).

2.1.1. Antitumour effect of Curcumin analogues on cancer cells in an MTT assay

The antitumour activity of Curcumin and BMAC compounds against MCF7 (human breast adenocarcinoma) and OVCAR-3 (human ovarian adenocarcinoma) cell lines was assessed *in vitro* using the MTT assay [68]. Cells were incubated for 72 h, (pH = 7.4, 37 °C, 5% CO_2), in the presence of each compound in the 0.5–35 μM concentration range. Compound **7** was observed to be about 4 times more toxic than Curcumin in both cell lines (Fig. 3). This result is in line with other studies in the literature that were performed on the same tumour cells [23,34]. In MCF7, the toxicity of BMAC **6a-c** and compound **8** are of the same order as shown by precursor compound **7**. In fact, the EC50 (half maximal effective concentration) of BMAC **6a-c** and compound **8**, reported in Table 1, are similar, and markedly lower (between 4 and 5.5 times) of the EC50 obtained with Curcumin. The substitution of one or two aromatic rings with carboranes does not modify the EC50 that was measured in the MCF7 cells. This observation is in agreement with the results reported in the literature about how the bioactivity shown by MAC compounds in which one or two aromatic rings were replaced with heterocyclic groups was maintained [27–58].

The cytotoxicity of both Curcumin and compound **7** against OVCAR-3 cells was much lower than against MCF7, which is in agreement with the results obtained by Suarez et al. [69] Accordingly, the EC50 that was obtained with BMAC **6a** and compound **8** (Table 1) have similar values. Interestingly, the most polar derivatives, BMAC **6b** and **6c**, showed lower EC50s that were similar to that of MCF7, which has proven itself to be the most promising for use in double therapy in combination with BNCT. Therefore, preliminary uptake studies were performed, using one of the most promising compounds, BMAC **6b**, in order to evaluate the amount of ^{10}B that is internalised by MCF7 and OVCAR-3. The uptake experiments were carried out by incubating cells for 24 h with BMAC **6b** at concentrations ranging from 0.6 to 13 μM. At the highest concentration, the amounts of ^{10}B that were internalised in the cells, measured by ICP-MS, were 5.7 and 21.3 ppm in MCF7 and OVCAR-3, respectively (see supplementary Fig. 1). BMAC **6b** contained natural abundance of boron isotopes.

2.1.2. Evaluation of the inhibition of Hen Egg White Lysozyme (HEWL) aggregate formation

The inhibition of the formation of fibril aggregates by BMAC **6a-c** was evaluated using the Thioflavin T fluorescent assay. Thioflavin T (ThT) is a dye that exhibits enhanced fluorescence (with excitation and emission at 440 and 490 nm, respectively) upon binding to fibril aggregates, and is used as a standard method to quantify the formation of amyloid or amyloid-like fibrils and to characterise potential inhibitors [70–72]. Hen Egg White Lysozyme (HEWL), a 14.3 kDa protein, is a highly stable and easily available water-soluble protein with four intrachain disulfide bonds [42]. The similar tertiary structures and function of human and hen egg white lysozymes makes HEWL a good model protein for amyloid aggregate formation [73]. The efficacy of **6a, 6b, 6c** and **8** in generating the disaggregation of HEWL fibrils was then

Table 1
The EC50 of Curcumin analogue compounds towards MCF7 and OVCAR-3 tumour cells.

Cells	Curcumin (μM)	Compound **7** (μM)	Compound **8** (μM)	Compound **6a** (μM)	Compound **6b** (μM)	Compound **6c** (μM)
MCF7	11 ± 4	2.9 ± 0.3	2.1 ± 0.2	2.9 ± 0.7	2.4 ± 0.5	2.6 ± 0.4
OVCAR-3	35 ± 5	6.4 ± 0.3	5.5 ± 0.2	4.1 ± 0.2	2.1 ± 0.2	1.8 ± 0.2

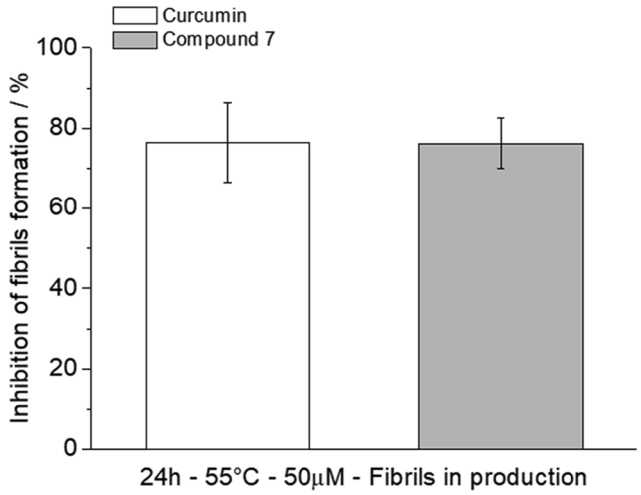

Fig. 4. Representative histogram comparing the inhibition of HEWL fibril formation (24 h, 55 °C) by compound **7** and Curcumin, as measured with a ThT fluorescence assay.

evaluated by means of the ThT fluorescence essay. HEWL (0.5 mg/mL) was incubated for 24 h at 55 °C and pH = 2 to induce fibril formation. First of all, the efficacy of reference compound **7** and Curcumin in the disaggregation of the formed fibrils was compared. To this purpose, the two compounds were incubated for 24 h during the HEWL fibril formation step. Fig. 4 shows that the % inhibition of fibril formation by compound **7** is comparable to that shown by Curcumin, thus confirming the maintenance of efficacy also in the mono-carbonyl analogue. Inhibition capacity was expressed as the percentage reduction in ThT fluorescence intensity compared to a control HEWL sample (w/o inhibitor compound) that was incubated under the same conditions.

Fig. 5 reports fluorescence intensities, measured at 490 nm, in the presence and in the absence of compounds **6a-c** and **8** in comparison with reference compound **7**. The inhibitory capacities of fibril formation were measured both during the occurrence of aggregate formation in the first 24 h (Fig. 5A), and after the incubation with pre-formed HEWL aggregates for another 24 h at 55 °C (Fig. 5B).

These preliminary experiments demonstrated that hybrid compound **6c** possesses enhanced efficacy in limiting the HEWL fibril aggregation process. This finding supports the view that the presence of two –OH groups enhances the binding efficacy of the inhibitor to HEWL fibril components.[35] The other interesting observation relates to the substitution, in chimeric derivatives **6a**, **6b**, of one of the two aromatic groups in compounds **7** with a carborane moiety, which led to a relatively low inhibition reduction of only 10–15%. This confirms the idea that carboranes can be considered to be analogous with aromatic groups, in this context, and that they can also maintain their inhibitory capacity in the absence of fundamental groups, such as –OH and $–OCH_3$. On the other hand, the substitution of both the aromatic groups with a carborane moiety (**8**) reduces inhibition potency to 10–20%. This demonstrates that only the presence of –OH group (probably with sufficient acidity) would be necessary to attain higher activity.

To get further support for the results obtained with ThT, a Congo Red (CR) fluorescence assay was also performed (Fig. 6). In fact, when CR binds to fibril aggregates, it gives a proportional increase in fluorescence, measured at 612 nm, when excited at 512 nm [74,75].

The assay was performed using pre-formed HEWL fibrils (1.5 mg/mL) that were prepared using the protocol for the ThT assay, as described above. Inhibition capacity was expressed as the percentage reduction in the CR fluorescence intensity of the treated samples (incubated with 100 μM inhibitors) compared to a control HEWL sample (w/o inhibitors), which was incubated under the same conditions.

Fig. 6 shows that the % fibril-formation inhibitions of compounds **7** and **6c** are not significantly different (p = 0.1644, Student *t*-test),

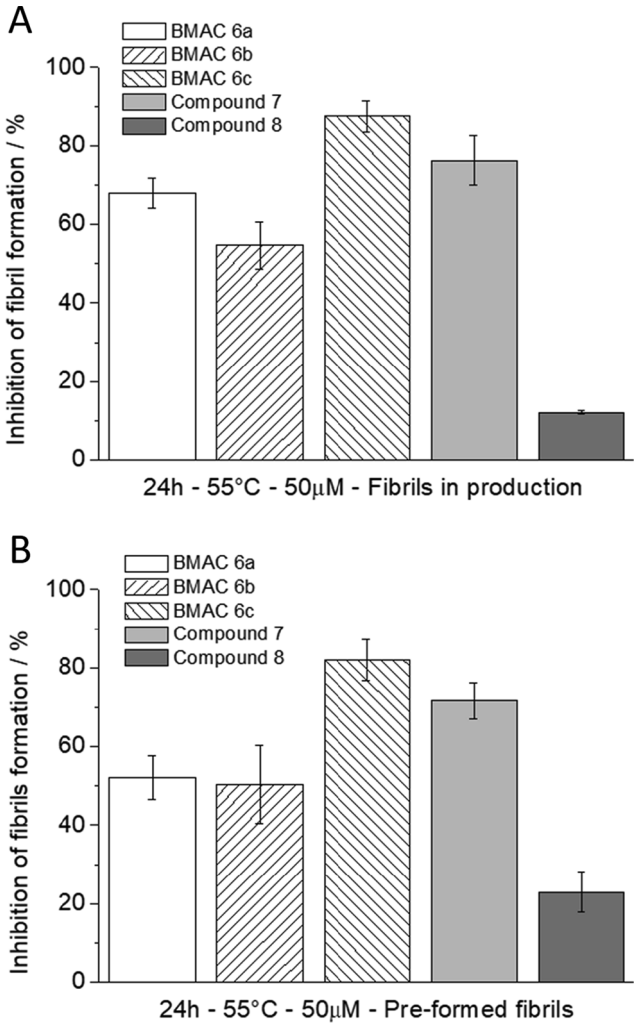

Fig. 5. Percentage inhibition of HEWL fibril formation as evaluated by incubating compounds **6a**, **6b**, **6c**, **7**, **8**: for 24 h at pH 2 and 55 °C with native HEWL (A) or for 24 h in the presence of pre-formed fibril aggregates (B).

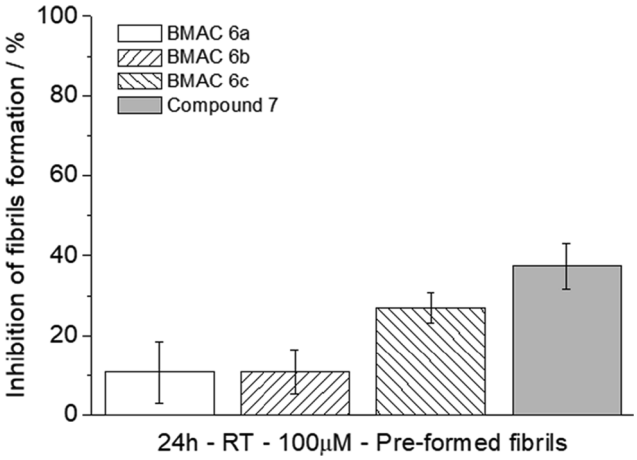

Fig. 6. Percentage inhibition of fibril formation, as evaluated by CR fluorescence assay. Compounds were incubated with pre-formed fibrils at t = 24 h for another 24 h at room temperature (RT).

whereas compounds **6a** and **6b** are less efficient. Although all % fibril-formation inhibitions are lower when measured with CR fluorescence, their trend appears to be in line with the results obtained using ThT, thus confirming that BMAC **6c** has a higher efficacy than **6a**, **6b** (Fig. 6).

2.1.3. Conclusions

We herein describe the synthesis and preliminary *in-vitro* tests of new boronated derivatives that have been used to improve the recognised efficacy of MAC thanks to the replacement of an aromatic ring with an *ortho*-carborane cage. These molecules were obtained in good yields by applying a relatively simple and straightforward synthetic approach. All derivatives that contained one or two carborane moieties showed significant cytotoxic activity, with EC50 values ranging from 1.8 to 5.5 μM. We can conclude that BMAC can be considered a new class of potential antineoplastic agent that can be used alone or in combination with BNCT. Water solubility and specific delivery to pathological tissues may be improved using specific carriers, such as cyclodextrins, liposomes, and polylactic and glycolic (PLGA) particles that can be further loaded with MRI contrast agents to allow real time, non-invasive boron quantification to be carried out before neutron irradiation. With regards to HEWL fibril aggregation, it has been found that the presence of at least one phenolic group in the molecule is important for the preservation of the inhibitory efficiency of these derivatives. Finally, the reported efficacy of the boronated Curcumin analogues in reducing lysozyme fibril formation, and the presence of boron atoms in the carborane cage will drive us to evaluate the feasibility of using BNCT as a radiative boost to enhance fibril disaggregation.

2.1.4. Experimental

2.1.4.1. General. Flasks and all equipment used for the generation and reaction of moisture-sensitive compounds were dried on an electric heater under Ar·THF and Et_2O were distilled from benzophenone ketyl, and CH_2Cl_2 from CaH_2 prior to use. BuLi (2.5 M in hexanes) was purchased from Aldrich. *Ortho*-carborane was bought from Katchem spol. s r. o. All commercially obtained reagents and solvents were used as received. Products were purified by preparative column chromatography on Macherey-Nagel silica gel for flash chromatography, 0.04–0.063 mm/230–400 mesh. When specified, silica gel is deactivated with 1% of Et_3N. Reactions were monitored by TLC using silica gel on TLC-PET foils, Fluka, 2–25 mm, layer thickness 0.2 mm, medium pore diameter 60 Å. Carboranes and their derivatives were visualized on TLC plates using a 5% $PdCl_2$ aqueous solution in HCl. ^{1}H NMR spectra were recorded at 200 MHz, ^{13}C NMR spectra at 50.2 MHz, ^{11}B NMR spectra at 64.1 MHz. Data were reported as follows: chemical shifts in ppm from tetramethylsilane as the internal standard, integration, multiplicity (s = singlet, d = doublet, t = triplet, q = quartet, dd = double–doublet, m = multiplet, br = broad), coupling constants (Hz), and assignment. ^{13}C and ^{11}B NMR spectra were recorded with complete proton decoupling. Chemical shifts were reported in ppm from the residual solvent as an internal standard. GC-MS spectra were obtained on a mass selective detector HP 5970B instrument operating at an ionizing voltage of 70 eV connected to a HP 5890 GC with a cross linked methyl silicone capillary column (25 m × 0.2 mm × 0.33 mm film thickness). ESI MS spectra were obtained on a LTQ Orbitrap high resolving power mass spectrometer (Thermo Scientific, Rodano, Italy), equipped with an atmospheric pressure interface and an ESI ion source. Samples were analyzed by flow injection at a 10 μL min^{-1} flow rate. The tuning parameters adopted for the ESI source were: source voltage 4.5 kV, capillary voltage 12.00 V, and tube lens voltage 55 V. The heated capillary temperature was maintained at 265 °C. The mass accuracy of the recorded ions (*vs.* the calculated ones) was ± 5 mmu (milli-mass units). Analyses were run using both full MS (50–2000 *m/z* range) and MS/MS acquisition in the positive and negative ion mode. IR spectra were recorded on a Perkin Elmer BX FT-IR. Synthesis of THP derivatives **2a-c** [76] and *C*-formyl-*ortho*carborane **1** [64] were carried out following the reported procedures.

B concentration was determined by inductively coupled plasma mass spectrometry (ICP-MS) (Element-2; Thermo-Finnigan, Rodano (MI), Italy) at medium mass resolution. Sample digestion was performed with 1 mL of concentrated HNO_3 (70%) using an high performance Microwave Digestion System (ETHOS UP Milestone, Bergamo, Italy). A natural abundance B standard solution was analysed during sample runs in order to check changing in the systematic bias. The calibration curve was obtained using four B absorption standard solutions (Sigma-Aldrich) in the range 0.2–0.01 μg/mL.

2.1.4.2. Cell Culture. Human MCF7 breast cancer cell line and human OVCAR-3 ovarian cancer cell line were purchased from American Type Culture Collection (ATCC, USA.) The MCF7 cells were cultured in EMEM (Lonza) supplemented with 10% (v/v) fetal bovine serum (FBS), 2 mM glutamine, 100 U/mL penicillin, 100 U/mL streptomycin, 1 mM sodium pyruvate, non-essential amino acids and 10 μg/mL insulin (Sigma). The OVCAR-3 cells were cultured in RPMI (Lonza) supplemented with 20% (v/v) FBS, 2 mM glutamine, 10 μg/mL insulin (Sigma), 100 U/mL penicillin and 100 U/mL streptomycin.

2.1.4.3. MTT assay. The MTT assay is based on the reduction of tetrazolium salts to formazan using mitochondrial succinate dehydrogenase, which is quantified by a spectrophotometer. MCF7 and OVCAR-3 cells were seeded at a density of 5×10^3 and 2.5×10^3 cells per well, respectively, in a 96-well microtiter plate. After 24 h at 37 °C and 5% CO_2, they were incubated with increasing concentration of compound 6a, 6b, 6c, 7, 8 and Curcumin for 72 h by adding stock solutions in dimethyl sulfoxide (DMSO). In all conditions the concentration during the cell incubation was maintained at 0.25% (v/v) in cell medium. After the incubation, the medium was removed and each well was incubated with thiazolyl blue tetrazolium bromide (Sigma) dissolved in the medium at a concentration of 0.45 mg/mL for 4 h at 37 °C and 5% CO_2. Then, after medium elimination, 150 μL of DMSO were added into each well to solubilize the formazan salt crystals produced by the metabolism of live cells and the microplate was incubated at room temperature (RT) for 30 min. Finally, absorbance was measured at 570 nm using an iMark microplate reader (Biorad). Cell vitality was reported as the percentage of dead cells observed in the treated samples relative to that observed in the non-treated control cells. The EC50 values of each compound were calculated by fitting the Dose Response MTT curve with a Origin 8 software using the equation: y = A1 + (A2-A1)/(1 + 10^((LOGx0-x)*p)) where A1 and A2 are bottom and top asymptote, respectively; LOGx0 and p are center and hill slope, respectively.

Thioflavin T (ThT) fluorescence assay. A standard fluorescent dye, ThT (Sigma), which exhibits a marked enhancement in its fluorescence intensity upon binding to amyloid structures, was used to detect the formation of HEWL fibrils. A stock solution of ThT (450 μM) was prepared in 95% (v/v) ethanol, and the concentration was determined spectrophotometrically using the molar extinction coefficient at 416 nm of 26,600 M^{-1} cm^{-1}. Phosphate buffered saline (PBS) was used to dissolve the ThT stock solution to obtain a ThT working solution at a concentration of 10 μM. Lysozyme from chicken egg white (Sigma) sample solutions (0.5 mg/mL) were prepared in 136.7 mM NaCl, 2.68 mM KCl and 1.54 mM NaN_3 (pH 2). To induce HEWL fibrils formation, lysozyme solution was incubated for 24 h at 55 °C, stirring (100 rpm). In order to access the inhibitory potency of fibrils formation, inhibitors compounds were incubated in lysozyme solution (4 mL) at a concentration of 50 μM (treated fibrils) dissolved in ethanol (5% v/v). A control lysozyme sample w/o inhibitors was prepared with 5% v/v ethanol (control fibrils). Furthermore, to access the disaggregation potency of inhibitors compounds, they were incubated at 50 μM concentration (5% v/v ethanol) for 24 h at 55 °C stirring (100 rpm) in the presence of pre-formed HEWL fibrils obtained after incubation of lysozyme (0.5 mg/mL) for 24 h at 55 °C pH = 2. At the end of the incubation, 80 μL of each sample were removed and were mixed thoroughly with ThT working solution (1920 μL) prior to measuring the ThT fluorescence intensities at 490 nm by exciting the samples at 440 nm via

Horiba Fluoromax 4 spectrofluorometer (Edison, USA). The % of inhibitory potency (% Inhibition) of fibril formation/disaggregation was calculated as follows:

% Inhibition = 100 × (ThT fluorescence intensity of control fibrils − ThT fluorescence intensity of treated fibrils)/ThT fluorescence intensity control fibrils).

Congo Red (CR) fluorescence assay. A stock solution of CR (Sigma) (300 μM) was prepared in 20 mM MES buffer pH 6, filtered with 0.2 um filter and the concentration was determined spectrophotometrically using the molar extinction coefficient at 505 nm of 59300 M^{-1} cm^{-1} diluting the stock solution 1:20 in sodium phosphate (1 mM, pH 7) and 40% ethanol. MES buffer pH 6 was used to dissolve the CR stock solution to obtain a CR working solution of 20 μM. To induce fibrils formation, HEWL sample solutions (1.5 mg/mL, 100 μM) were incubated in 136.7 mM NaCl, 2.68 mM KCl and 1.54 mM NaN_3 (pH 2) for 24 h at 55 °C, stirring (100 rpm). To access the disaggregation potency of compound 6a, 6b, 6c, 7, they were incubated at 100 μM concentration (5% v/v ethanol) (treated fibrils) for 24 h RT in the presence of preformed HEWL fibrils prepared in NaCl/KCl/NaN_3 buffer pH 2. A control fibrils sample w/o inhibitors was prepared with 5% v/v ethanol (control fibrils). At the end of the incubation, 200 ul of each sample were removed and were mixed thoroughly with or w/o CR working solution such that the final protein concentration became 10 μM and CR 20 μM. After 15 min of incubation at RT, the fluorescence intensities were measured at 612 nm by exciting the samples at 512 nm via Horiba Fluoromax 4 spectrofluorometer (Edison, USA). The excitation and emission slit widths were 2.5 and 5.0 nm, respectively. The % of inhibitory potency of fibril disaggregation was calculated as follows:

The CR fluorescence intensity of control and treated samples were calculated by subtracting the intrinsic fluorescence intensity (w/o CR) to their intensity fluorescence in the presence of CR.

The percentage reduction in CR fluorescence intensity = 100 × (CR fluorescence intensity of control fibrils–CR fluorescence intensity of treated fibrils)/CR fluorescence intensity control fibrils).

2.2. Chemistry

General procedures for the synthesis of chalcones (4a-c). The appropriate THP-protected phenylaldehyde (**2a-c**, 1 eq.) was dissolved in acetone then added dropwise to a solution of NaOH (1.5 eq.) in 3 mL of water and the resulting mixture stirred overnight at room temperature. The reaction was then cooled to 0 °C then added to a 25 mL solution of ice and water and vigorously stirred for 10 min. The precipitated yellowish solid was filtered, washed with cold water, dried and purified by column chromatography on deactivated silica gel. The solid obtained was then crystallized from MeOH to yield the desired product.**

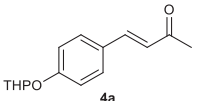

4a

(3*E*)-4-(4-((tetrahydro-2*H*-pyran-2-yl)oxy)phenyl)but-3-en-2-one (4a). According to the described general procedure, 4-((tetrahydro-2*H*-pyran-2-yl)oxy)benzaldehyde **5** (4.20 g, 20.4 mmol) was reacted with acetone (20 mL) and NaOH (1.20 g, 30.0 mmol) to obtain a crude yellow solid, purified on silica gel (EP/EE 50/50) and crystalized from MeOH to yield the solid product as needle-shaped white crystals (4,18 gr, 85%). ^{1}H NMR (600 MHz, $CDCl_3$): *δ* 7.48 (d, *J* = 16.2 Hz, 1H, CO−CH=C*H*), 7.46 (d, *J* = 8.6 Hz, 2H, Ar*H*), 7.05 (d, *J* = 8.6 Hz, 2H, Ar*H*), 6.61 (d, *J* = 16.2 Hz, 1H, CO−C*H*=CH), 5.47 (t, *J* = 3.1 Hz, 1H, OC*H*O), 3.86 (m, 1H, OCH_{2a}) 3.61 (m, 1H, OCH_{2b}), 2.36 (s, 3H, COCH_3), 2.10–1.80 (m, 3H, CH−CH_2−CH_2), 1.80–1.55 (m, 3H, CH_2−CH_2−CH_2). ^{13}C NMR (150 MHz, $CDCl_3$): 198.5 (Cq), 159.2 (Cq), 143.4 (CH), 129.9 (CH), 127.8 (Cq), **125.3 (CH), 116.8 (CH), 96.2 (CH), 62.1 (CH_2), 30.2 (CH_2), 27.5 (CH_3) 25.2** (CH_2), 18.7 (CH_2). ν_{max} (neat)/cm^{-1}: 2993, 2948, 2896, 2845, 1689, 1592, 1110, 951, 806. m.p.: 78–80 °C. ESI HRMS for $C_{15}H_{18}O_3$ Calcd. $[M + H]^+$: 247.1334 Found: 247.1356 $[M+H]^+$.

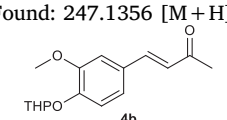

4b

(3*E*)-4-(3-methoxy-4-((tetrahydro-2*H*-pyran-2-yl)oxy)phenyl)but-3-en-2-one (4b) [77]. According to the described general procedure, 3-methoxy-4-((tetrahydro-2*H*-pyran-2-yl)oxy)benzaldehyde **2b** (4.00 g, 16.9 mmol) was reacted with acetone (17 mL) and NaOH (1.00 g, 25.0 mmol) to obtain a crude yellow solid, purified on deactivated flash silica gel (EP/EE 50/50) and crystalized from MeOH to yield the product as pale yellow crystalline solid (4.21 gr, 90%). ^{1}H NMR (200 MHz, $CDCl_3$): *δ* 7.46 (d, *J* = 15.6 Hz, 1H, CO−CH=C*H*), 7.14 (m, 1H, Ar*H*), 7.10 (m, 2H, Ar*H*), 6.60 (d, *J* = 15.6 Hz, 1H, CO−C*H*=CH), 5.49 (t, *J* = 3.0 Hz, 1H, OC*H*O), 3.91 (s, 3H, OCH_3), 4.10–3.95 (m, 1H, OCH_{2a}), 3.75–3.59 (m, 1H, OCH_{2b}), 2.38 (s, 3H, COCH_3), 2.03–1.88 (m, 3H, CH−CH_2−CH_2), 1.75–1.57 (m, 3H, CH−CH_2−CH_2).

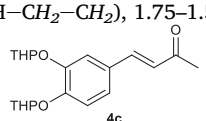

4c

(3*E*)-4-(3,4-bis((tetrahydro-2*H*-pyran-2-yl)oxy)phenyl)but-3-en-2-one (4c). According to the described general procedure, 3,4-bis((tetrahydro-2*H*-pyran-2-yl)oxy)benzaldehyde **6** (3.00 g, 9.79 mmol) was reacted with acetone (10 mL) and NaOH (0.60 g, 15.0 mmol). Acetone was removed under reduced pressure. AcOEt (20 mL) was added to the resulting aqueous solution and the obtained mixture vigorously stirred for 30 min. The organic phase was separated, washed with brine (2x15 mL), dried with sodium sulfate and filtered. The solvent was removed under reduced pressure to obtain a yellow oil, purified on silica gel (EP/AcOEt 75/25) to yield the product as a colorless oil (2.91 gr, 86%). Mixture of isomers. ^{1}H NMR (600 MHz, $CDCl_3$): *δ* 7.42 (d, *J* = 16.2 Hz, 1H, CO−CH=C*H*), 7.32 (m, 1H, Ar*H*), 7.12 (m, 2H, Ar*H*), 6.56 (d, *J* = 16.2 Hz, 1H, CO−C*H*=CH), 5.48 (t, *J* = 2.4 Hz, 1H, OC*H*O, isomer 1), 5.46 (t, *J* = 2.4 Hz, 1H, OC*H*O, isomer 2), 5.43 (t, *J* = 3.0 Hz, 1H, OC*H*O, isomer 3), 5.41 (t, *J* = 3.0 Hz, 1H, OC*H*O, isomer 4), 3.97 (m, 1H, OCH_{2a}, isomer 1) 3.90 (m, 1H, OCH_{2a}, isomer 1), 3.59 (m, 2H, OCH_2, isomer 2), 2.32 (s, 3H, CO−CH_3), 2.05–1.80 (m, 6H, CH−CH_2−CH_2), 1.75–1.55 (m, 6H, CH_2−CH_2−CH_2). ^{13}C NMR (150 MHz, $CDCl_3$): 198.5 (Cq), 150.0 (Cq), 149.7 (Cq), 147.6 (Cq), 147.4 (Cq), 143.6 (CH), 143.5 (CH), 128.8 (CH), 128.7 (CH), 125.8 (CH), 125.7 (CH), 123.9 (CH), 123.8 (CH), 118.1 (CH), 117.8 (CH), 117.7 (CH), 117.6 (CH), 97.9 (CH), 97.4 (CH), 97.3 (CH), 96.8 (CH), 62.1 (CH_2), 62.0 (CH_2), 61.9 (CH_2), 61.8 (CH_2), 30.4 (CH_2), 30.4 (CH_2), 30.3 (CH_2), 30.2 (CH_2), 27.4 (CH_3) 25.3 (CH_2), 25.3 (CH_2), 18.6 (CH_2), 18.6 (CH_2), 18.5 (CH_2). ν_{max} (neat)/cm^{-1}: 2942, 2871, 2854, 1663, 1504, 1255, 954, 918. ESI HRMS for $C_{20}H_{26}O_5$ Calcd. $[M+H]^+$: 347.1858 Found: 347.1833 $[M+H]^+$.

General procedure for the aldol condensation between *C*-formyl-*ortho*-carborane and chalcones. In a 10 mL dried Schlenk bottle under nitrogen atmosphere, the appropriate chalcone (**4a-c**, 1 eq., 1.00 mmol) was dissolved in the minimal amount of THF and cooled to −78 °C. In another dried round bottomed Schlenk bottle under N_2, freshly distilled diisopropylamine (1.1 eq., 1.54 mL, 1.10 mmol) and 5 mL of THF were added and the mixture was stirred and cooled to −10 °C. *n*-BuLi (1.1 eq., 0.44 mL, 1.10 mmol) was then slowly added for 10 min. Stirring was continued at −10 °C for 30 min to obtain the lithium diisopropylamine LDA base solution. The mixture was then cooled to −78 °C and the chalcone solution was dropwise added to the LDA solution. Stirring was continued at −78 °C for 3.5 h then *C*-formyl-*ortho*-carborane **1** (1.2 eq., 0.210 g, 1.20 mmol) was added in one portion. The reaction was stirred until total disappearance of the chalcone spot on TLC plate, allowing the temperature to raise to a maximum of −50 °C. The process was then quenched adding 10 mL of water and diluting the solution with 15 mL of Et_2O. The resulting mixture was stirred for 20 min at 0 °C. The organic phase was separated,

and the aqueous phase extracted with 10 mL portions of AcOEt until it became colorless again. The organic phases, dried over Na_2SO_4 were filtered and the solvent removed under reduced pressure to yield a crude solid that was then purified by column chromatography on deactivated silica gel.

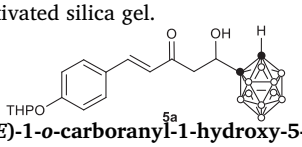

5a

(4*E*)-1-*o*-carboranyl-1-hydroxy-5-(4-((tetrahydro-2*H*-pyran-2-yl) oxy)phenyl)pent-4-en-3-one (5a). Following the reported procedure, chalcone **4a** was reacted with LDA and formyl-*o*-carborane **1** affording 232 mg of a yellow solid (EP/AcOEt 70/30, 55%). ^{1}H NMR (600 MHz, CD_3OCD_3): δ 7.64 (d, J = 6.0 Hz, 2H, Ar−*H*), 7.63 (d, J = 16.2 Hz, 1H, ArC*H*=CH−CO), 7.07 (d, J = 6.0 Hz, 2H, Ar*H*), 6.77 (d, J = 16.2 Hz, 1H, ArCH=C*H*CO), 5.57 (d, J = 6.2 Hz, 1H, CH_2−CH(O*H*)−C), 5.54 (t, J = 3.1 Hz, 1H, OC*H*O), 4.80 (ddd, J = 9.3 Hz, J = 6.2 Hz, J = 3.0 Hz, 1H, C*H*OH), 4.73 (s, 1H, $B_{10}H_{10}CH$), 3.81 (m, 1H, OCH_{2a}) 3.59 (m, 1H, OCH_{2b}), 3.12 (dd, J = 16.5 Hz, J = 9.3 Hz, 1H, CH_{2a}CH(OH)C), 3.04 (dd, J = 16.5 Hz, J = 3.0 Hz, 1H, CH_{2b}CH(OH)−C), 2.79–1.91 (m, 10*H*, B*H*), 1.84 (m, 3H, CH−CH_2−CH_2), 1.74–1.58 (m, 3H, CH_2−CH_2−CH_2). ^{13}C NMR (150 MHz, CD_3OCD_3): δ 196.8 (Cq), 160.3 (Cq), 143.9 (CH), 130.9 (CH), 128.8 (Cq), 125.1(CH), 117.6 (CH), 96.9 (CH), 81.1 (Cq), 69.37 (CH), 62.5 (CH_2), 60.9 (CH), 47.8 (CH_2), 30.1(CH_2), 25.02(CH_2), 19.4 (CH_2). ^{11}B NMR (192.5 MHz, CD_3OCD_3): −4.7, −5.9, −10.4, −12.9, −14.1, −14.8. Mp: degradation 155–156 °C ν_{max} (neat)/cm^{-1}: 3365, 3087, 2947, 2866, 2589, 1679, 1590, 1512, 1242, 1102, 1072, 950, 909. ESI HRMS for $C_{14}H_{30}B_{10}O_4$ Calcd 421.3075 $[M+H]^+$, Found: 421.3071 $[M+H]^+$

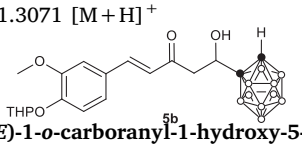

5b

(4*E*)-1-*o*-carboranyl-1-hydroxy-5-(3-methoxy-4-((tetrahydro-2*H*-pyran-2-yl)oxy)phenyl)pent-4-en-3-one (5b). Following the reported procedure, chalcone **4b** was reacted with LDA and formyl-*o*-carborane **1** affording 234 mg of a yellow solid (EP/AcOEt 75/25, 54%). ^{1}H NMR (600 MHz, CD_3OCD_3): δ 7.65 (d, J = 18.0 Hz, 1H, ArC*H*=CHCO), 7.38 (bs, 1H, Ar*H*), 7.24 (dd, J = 6.0 Hz, J = 1.0 Hz, 1H, Ar*H*), 7.17 (bd, J = 6.0 Hz, 1H, Ar*H*), 6.83 (d, J = 18.0 Hz, 1H, ArCH=C*H*CO), 5.57 (d, J = 6.0 Hz, 1H, CH_2−CH(O*H*)−C), 5.51 (t, J = 6.0 Hz, 1H, OC*H*O), 4.79 (ddd, J = 9.3 Hz, J = 6.2 Hz, J = 3.0 Hz, 1H, C*H*OH), 4.73 (s, 1H, $B_{10}H_{10}CH$), 3.89 (3H, s, OCH_3), 3.86 (m, 1H, OCH_{2a}) 3.56 (m, 1H, OCH_{2b}), 3.12 (dd, J = 18.0 Hz, J = 12.0 Hz, 1H, CH_{2a}CH(OH)), 3.03 (dd, J = 18.0 Hz, J = 3.0 Hz, 1H, CH_{2b}CH(OH)), 2.80–1.90 (m, 10*H*, B*H*), 1.85 (m, 3H, CH−CH_2−CH_2), 1.70–1.55 (m, 3H, CH_2−CH_2−CH_2).^{13}C NMR (150 MHz, CD_3OCD_3): δ 196.8 (Cq), 151.5 (Cq), 149.9 (Cq), 144.4 (CH), 129.5 (Cq), 125.4 (CH), 123.7(CH), 117.8 (CH), 112.3 (CH), 97.7 (CH), 73.1 (Cq), 69.4 (CH), 62.4 (CH_2), 60.9 (CH), 56.4 (CH_3), 47.8 (CH_2), 30.9 (CH_2), 25.9 (CH_2), 19.4 (CH_2). ^{11}B NMR (192.5 MHz, CD_3OCD_3)-4.7, −6.0, −10.5, −13.0, −14.1, −14.8. Mp: degradation 154–157 °C. ν_{max} (neat)/cm^{-1}: 3392, 3085, 2946, 2878, 2577, 1581, 1510, 1254, 1112, 1022, 950, 912. ESI HRMS for $C_{19}H_{33}B_{10}O_5$ Calcd 451.3559 $[M+H]^+$, Found: 451.33563 $[M+H]^+$

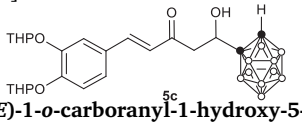

5c

(4*E*)-1-*o*-carboranyl-1-hydroxy-5-(3,4-bis((tetrahydro-2*H*-pyran-2-yl)oxy)phenyl)pent-4-en-3-one (5c). Following the reported procedure, chalcone **4c** was reacted with LDA and formyl-*o*-carborane affording 265 mg of a yellow solid (EP/AcOEt 75/25, 51%). Mixture of isomers. ^{1}H NMR (600 MHz, CD_3OCD_3): δ 7.63 (d, J = 16.2 Hz, 1H, ArC*H*=CHCO), 7.50 (d, J = 1.8 Hz, 1H, Ar*H*), 7.31 (dq, J = 7.8 Hz, 3.0 Hz, 1H, Ar*H*), 7.20 (dd, J = 7.8 Hz, 1H, Ar*H*), 6.77 (d, J = 16.2 Hz, 1H, ArCH=C*H*CO), 5.56 (m, 2H, OC*H*O, O*H*), 4.79 (ddd, J = 9.0, 6.0, 3.0 Hz, 1H, C*H*OH), 4.73 (bs, 1H, $B_{10}H_{10}CH$), 3.97 (td, J = 10.8, 3.0 Hz, 1H, O−$CH_{2axial,}$ isomer a), 3.90 (tt, J = 10.2, 3.0 Hz, 1H, O−$CH_{2equat.}$ isomer a), 3.58 (m, 2H, O$CH_{2,}$ isomer b), 3.12 (dd, J = 16.8, 9.6, Hz, 1H, CH_{2a}CHOH isomer a), 3.10 (dd, J = 16.8, 9.6, Hz, 1H, CH_{2a}CHOH isomer b), 3.04 (dd, J = 16.8, 3.0 Hz, 1H, CH_{2b}CHOH isomer a), 3.02 (dd, J = 16.8, 3.0 Hz, 1H, CH_{2b}CHOH isomer b), 2.10–1.20 (m, 10*H*, B*H*), 1.86 (m, 6H, CH−CH_2−CH_2), 1.64 (m, 6H, CH_2−CH_2−CH_2).^{13}C NMR (150 MHz, CD_3OCD_3): δ 196.8 (Cq), 151.1 (Cq), 151.0 (Cq), 148.4 (Cq), 148.3 (Cq), 148.3 (CH), 144.2 (CH), 144.2 (CH), 129.4 (Cq), 129.3 (Cq), 125.5 (CH), 124.8 (CH), 124.6 (Cq), 124.0 (CH), 123.9 (CH), 118.9 (CH), 118.9 (CH), 118.6 (CH), 118.5 (CH), 118.5 (CH), 118.3 (CH), 98.1 (CH), 97.7 (CH), 97.6 (CH), 97.4 (CH), 81.1 (Cq), 69.4 (CH), 69.4 (CH), 62.4 (CH_2), 62.3 (CH_2), 62.2 (CH_2), 62.2 (CH_2), 60.9 (CH), 47.7 (CH_2), 47.7 (CH_2), 31.0 (CH_2), 31.0 (CH_2), 31.0 (CH_2), 30.9 (CH_2), 26.0 (CH_2), 25.9 (CH_2), 19.3 (CH_2), 19.2 (CH_2), 19.2 (CH_2). ^{11}B NMR (192.5 MHz, CD_3OCD_3): −4.7, −5.9, −10.5, −12.9, −14.2, −14.8. Mp: degradation 156–157 °C. ν_{max} (neat)/cm^{-1}: 3392, 3085, 2932, 2872, 2583, 1580, 1508, 1260, 1108, 1054, 953, 910. ESI HRMS for $C_{23}H_{38}B_{10}O_6$ Calcd 521.3677 $[M+H]^+$, Found: 521.3673 $[M+H]^+$

General procedure for the dehydration of aldol carborane-derivatives. A 0.05 M solution of the appropriate aldol condensation product (**5a-c**) in THF was reacted with a 10% w/w solution of H_2SO_4 in water. The resulting mixture was vigorously stirred and heated to reflux for 36 h, then cooled to room temperature and diluted with water. The organic phase was separated, and the aqueous phase extracted with 10 mL portions of AcOEt, then dried over Na_2SO_4, filtered and the solvent removed under reduced pressure to yield a crude solid that was then purified by column chromatography on silica gel.

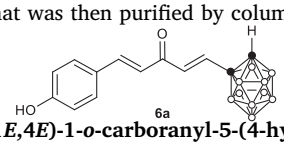

6a

(1*E*,4*E*)-1-*o*-carboranyl-5-(4-hydroxyphenyl)penta-1,4-dien-3-one (6a). Following the reported procedure, aldol **5a** (100 mg, 0.24 mmol) was treated with H_2SO_4 affording 46 mg of a yellow solid (EP/AcOEt 60/40, 45%). ^{1}H NMR (600 MHz, CD_3OCD_3): δ 9.03 (s, 1H, ArO*H*), 7.70 (d, J = 16.2 Hz, 1H, ArC*H*=CHCO), 7.59 (dm, J = 8.4 Hz, 2H, Ar*H*), 7.03 (d, J = 15.6 Hz, 1H, CO−C*H*=CH−$CB_{10}H_{10}$), 6.96 (d, J = 15.6 Hz, COCH=C*H*$CB_{10}H_{10}$), 6.94 (d, J = 16.2 Hz, 1H, ArCH=C*H*CO), 6.88 (dm, J = 8.4 Hz, 2H, Ar−*H*), 4.99 (s, 1H, $B_{10}H_{10}CH$), 2.82–1.70 (m, 10H, B*H*). ^{13}C NMR (150 MHz, CD_3OCD_3): δ 187.0 (Cq), 161.3 (Cq), 145.8 (CH), 137.2 (CH), 134.4 (CH), 131.7 (CH), 127.1 (Cq), 123.0 (CH), 116.9 (CH), 73.9 (Cq), 62.0 (CH). ^{11}B NMR (192.5 MHz, CD_3OCD_3): −3.7, −5.4, −9.9, −11.9, −12.4, −13.8

Mp: degradation 154–155 °C. ν_{max} (neat)/cm^{-1}: 3453, 2920, 2582, 1560, 1278, 970. ESI HRMS for $C_{13}H_{20}B_{10}O_2$ Calcd: 319.2372 $[M+H]^+$, Found: 319.2397 $[M+H]^+$

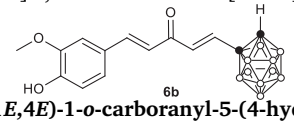

6b

(1*E*,4*E*)-1-*o*-carboranyl-5-(4-hydroxy-3-methoxyphenyl)penta-1,4-dien-3-one (6b). Following the reported procedure, aldol **5b** (107 mg, 0.24 mmol) was treated with H_2SO_4 affording 58 mg of a yellow solid (EP/AcOEt 75/25, 70%). ^{1}H NMR (600 MHz, CD_3OCD_3): δ 8.33 (s, 1H, ArO*H*), 7.72 (d, J = 16.2 Hz, 1H, ArC*H*=CHCO), 7.38 (d, 1H, J = 1.8 Hz, Ar*H*), 7.24 (dd, J = 7.8, 1.8 Hz, 1H, Ar*H*), 7.05 (d, J = 15.0 Hz, 1H, COC*H*=CH$CB_{10}H_{10}$), 6.99 (d, J = 16.2 Hz, 1H, ArCH=C*H*CO), 6.97 (d, J = 15.0 Hz, 1H, COCH=C*H*$CB_{10}H_{10}$), 6.89 (d, J = 8.4 Hz, 1H, Ar−*H*), 4.99 (s, 1H, $B_{10}H_{10}CH$), 3.91 (s, 3H, OCH_3), 2.79–1.95 (m, 10*H*, B*H*). ^{13}C NMR (150 MHz, CD_3OCD_3): δ 186.9 (Cq), 150.9 (Cq), 148.8 (Cq), 146.2 (CH), 137.2 (CH), 134.2 (CH), 127.5 (Cq), 124.8 (CH) 123.4 (CH), 116.3 (CH), 111.8 (CH), 73.8 (Cq), 62.1 (CH), 56.4 (CH_3). ^{11}B NMR (192.5 MHz, CD_3OCD_3): −3.7, −5.4, −10.0, −12.1, −12.2, −13.8. Mp: degradation 154–156 °C. ν_{max} (neat)/cm^{-1}: 3223, 3058, 2955, 2925, 2586, 1656, 1580, 1511, 1171, 821, 721. ESI HRMS for $C_{14}H_{22}B_{10}O_3$ Calcd 349.2568 $[M+H]^+$, Found:

349.2532 $[M+H]^+$

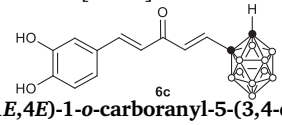

6c

(1*E*,4*E*)-1-*o*-carboranyl-5-(3,4-dihydroxyphenyl)penta-1,4-dien-3-one (6c). Following the reported procedure, aldol **5c** (125 mg, 0.24 mmol) was treated with H_2SO_4 affording 54 mg of a yellow solid (EP/Acetone 67/33, 68%). ^{1}H NMR (600 MHz, CD_3OCD_3): 8.50 (bs, 2H, ArO*H*), 7.66 (d, J = 15.9 Hz, 1H, ArC*H*=CHCO), 7.19 (d, J = 1.9 Hz, 1H, Ar*H*), 7.09 (dd, J = 1.9, J = 8.2, 1H, Ar*H*), 7.01 (d, J = 15.4 Hz, 1H, COC*H*=CHC$B_{10}H_{10}$), 6.96 (d, J = 15.4 Hz, 1H, COCH=C*H*C$B_{10}H_{10}$), 6.89 (d, J = 15.9 Hz, 1H, ArCH=C*H*CO) 6.86 (d, J = 8.2, 1H, Ar*H*), 4.95 (s, 1H, $B_{10}H_{10}$C*H*), 2.98–1.80 (m, 10*H*, B*H*). ^{13}C NMR (150 MHz, CD_3OCD_3): 187.0 (Cq), 149.5 (Cq), 146.4 (Cq), 146.2 (CH), 137.2 (CH), 134.4 (CH), 127.8 (Cq), 123.5 (CH), 123.0 (CH), 116.5 (CH), 115.6 (CH), 73.9 (Cq), 62.0 (CH). ^{11}B NMR (192.5 MHz, CD_3OCD_3): −3.7, −5.4, −10.0, −12.0, −12.4, −13.8. Mp: degradation 155–156 °C. ν_{max} (neat)/cm^{-1}: 3454, 3213, 3052, 2919, 2582, 1556, 1278, 1184, 970. ESI HRMS for $C_{13}H_{20}B_{10}O_3$ Calcd: 335.2421 $[M+H]^+$, Found: 335.2401 $[M+H]^+$

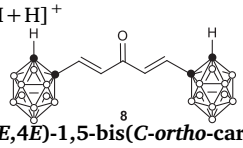

8

(1*E*,4*E*)-1,5-bis(*C*-*ortho*-carboranyl)penta-1,4-dien-3-one (8) In a screw cap reaction vessel, dried and under nitrogen atmosphere, *C*-formyl-*ortho*-carborane (0.172 g, 1.00 mmol) and $LiClO_4$ (0.106 g, 1.00 mmol) were dissolved in 3 mL of anhydrous toluene. Then, 1 eq. of acetone (0.074 mL, 0.058 g, 1.00 mmol) and 0.1 eq of Et_3N (0.014 mL, 0.010 g, 0.10 mmol) were added, then the vessel was closed and the stirred reaction warmed to 112 °C for 5 days. The reaction was cooled to rt and diluted with DCM then 20 mL of water were added, the organic phases washed with a saturated solution of NH_4Cl, dried and the solvent evaporated. The crude was purified by column chromatography affording 0.036 g of (1*E*,4*E*)-1,5-bis(*C*-*ortho*-carboranyl)penta-1,4-dien-3-one **(8)** as a white solid (EP/AcOEt 85/15, 10%). ^{1}H NMR (600 MHz, $CDCl_3$): 6.80 (d, J = 15.4 Hz, 2H, C*H*=CHC$B_{10}H_{10}$), 6.59 (d, J = 15.4 Hz, 2H, CH=C*H*C$B_{10}H_{10}$), 3.70 (s, 2H, $B_{10}H_{10}$C*H*), 3.50–1.00 (m, 20H, B*H*). ^{13}C NMR (150 MHz, CD_3OCD_3): 184.4 (Cq), 138.9 (CH), 132.3 (Cq), 71.10 (Cq), 59.9 (CH). ^{11}B NMR (192.5 MHz, $CDCl_3$): −2.8, −4.2, −9.3, −11.9, −12.7, −13.7. Mp: 215–218 °C. ν_{max} (neat)/cm^{-1}: 3065, 2578, 1640, 965, 721. ESI *m/z* 368 $[M+H]^+$. ESI HRMS for $C_9H_{26}B_{20}O$ Calcd: 372.4001 $[M+H]^+$, Found: 372.3993 $[M+H]^+$

Declaration of Competing Interest

The authors declare that they have no known competing financial interests or personal relationships that could have appeared to influence the work reported in this paper.

Acknowledgements

We thank Silvio Aime for the fruitful discussion. This work has received funding from the project: “L'Oréal Italia per le Donne e la Scienza” and from “Ricerca Locale of University of Torino”. This work was performed in the framework of the Consorzio CIRCMSB.

Appendix A. Supplementary material

Supplementary data to this article can be found online at https://doi.org/10.1016/j.bioorg.2019.103324.

References

[1] S. Vahid, S. Amirhossein, H. Hossein, Turmeric (Curcuma longa) and its major constituent (Curcumin) as nontoxic and safe substances: review, Phytother. Res. 32 (6) (2018) 985–995.
[2] I.W. Hamley, Peptide Fibrillization, Angew. Chem., Int. Ed. Engl. 46 (43) (2007) 8128–8147.
[3] M. Heger, R.F. van Golen, M. Broekgaarden, M.C. Michel, The molecular basis for the pharmacokinetics and pharmacodynamics of curcumin and its metabolites in relation to cancer, Pharmacol. Rev. 66 (1) (2014) 222–307.
[4] F. Shahabipour, M. Caraglia, M. Majeed, G. Derosa, P. Maffioli, A. Sahebkar, Naturally occurring anti-cancer agents targeting EZH2, Cancer Lett. 400 (2017) 325–335.
[5] Y.Y. Li, J. Yang, H.W. Liu, J. Yang, L. Du, H.W. Feng, Y.L. Tian, J.Q. Cao, C.Z. Ran, Tuning the stereo-hindrance of a Curcumin scaffold for the selective imaging of the soluble forms of amyloid beta species, Chem. Sci. 8 (11) (2017) 7710–7717.
[6] F. Mohammadi, A. Mahmudian, M. Moeeni, L. Hassani, Inhibition of amyloid fibrillation of hen egg-white lysozyme by the natural and synthetic Curcuminoids, RSC Adv. 6 (28) (2016) 23148–23160.
[7] M. Venigalla, S. Sonego, E. Gyengesi, M.J. Sharman, G. Münch, Novel promising therapeutics against chronic neuroinflammation and neurodegeneration in Alzheimer's disease, Neurochem. Int. 95 (2016) 63–74.
[8] A. Battisti, A. Palumbo Piccionello, A. Sgarbossa, S. Vilasi, C. Ricci, F. Ghetti, F. Spinozzi, A. Marino Gammazza, V. Giacalone, A. Martorana, A. Lauria, C. Ferrero, D. Bulone, M.R. Mangione, P.L. San Biagio, M.G. Ortore, Curcumin-like compounds designed to modify amyloid beta peptide aggregation patterns, RSC Adv. 7 (50) (2017) 31714–31724.
[9] R.M.C. Di Martino, A. Bisi, A. Rampa, S. Gobbi, F. Belluti, Recent progress on Curcumin-based therapeutics: a patent review (2012–2016). Part II: Curcumin derivatives in cancer and neurodegeneration, Expert Opin. Ther. Pat. 27 (8) (2017) 953–965.
[10] K.M. Nelson, J.L. Dahlin, J. Bisson, J. Graham, G.F. Pauli, M.A. Walters, The essential medicinal chemistry of curcumin, J. Med. Chem. 60 (5) (2017) 1620–1637.
[11] M.A. Tomren, M. Másson, T. Loftsson, H.H. Tønnesen, Studies on Curcumin and Curcuminoids: XXXI. Symmetric and asymmetric Curcuminoids: Stability, activity and complexation with cyclodextrin, Int. J. Pharm. 338 (1) (2007) 27–34.
[12] M.J.C. Rosemond, L. St, T. John-Williams, T. Yamaguchi, J.S. Walsh Fujishita, Enzymology of a carbonyl reduction clearance pathway for the HIV integrase inhibitor, S- 1360: role of human liver cytosolic aldo-keto reductases, Chem. Biol. Interact. 147 (2) (2004) 129–139.
[13] G. Grogan, Emergent mechanistic diversity of enzyme-catalysed β-diketone cleavage, Biochem. J. 388 (3) (2005) 721–730.
[14] B. Kumar, V. Singh, R. Shankar, K. Kumar, R.K. Rawal, Synthetic and medicinal prospective of structurally modified curcumins, Curr. Top. Med. Chem. 17 (2) (2017) 148–161.
[15] X. Fang, L. Fang, S. Gou, L. Cheng, Design and synthesis of dimethylaminomethyl-substituted Curcumin derivatives/analogues: Potent antitumor and antioxidant activity, improved stability and aqueous solubility compared with Curcumin, Bioorg. Med. Chem. Lett. 23 (5) (2013) 1297–1301.
[16] G.K. Samra, K. Dang, H. Ho, A. Baranwal, J. Mukherjee, Dual targeting agents for Aβ plaque/P-glycoprotein and Aβ plaque/nicotinic acetylcholine α4β2* receptors—potential approaches to facilitate Aβ plaque removal in Alzheimer's disease brain, Med. Chem. Res. 27 (6) (2018) 1634–1646.
[17] C. Zhuang, W. Zhang, C. Sheng, W. Zhang, C. Xing, Z. Miao, Chalcone: a privileged structure in medicinal chemistry, Chem. Rev. 117 (12) (2017) 7762–7810.
[18] M. Gomes, E. Muratov, M. Pereira, J. Peixoto, L. Rosseto, P. Cravo, C. Andrade, B. Neves, Chalcone derivatives: promising starting points for drug design, Molecules 22 (8) (2017) 1210.
[19] Z. Nowakowska, A review of anti-infective and anti-inflammatory chalcones, Eur. J. Med. Chem. 42 (2) (2007) 125–137.
[20] S.L. Gaonkar, U.N. Vignesh, Synthesis and pharmacological properties of chalcones: a review, Res. Chem. Intermed. 43 (11) (2017) 6043–6077.
[21] F.C. Rodrigues, N.V. Anilkumar, G. Thakur, Developments in the anticancer activity of structurally modified curcumin: an up-to-date review, Eur. J. Med Chem (2019).
[22] Y.L. Zhang, X. Jiang, K.S. Peng, C.W. Chen, L.L. Fu, Z. Wang, J.P. Feng, Z.G. Liu, H.J. Zhang, G. Liang, Z. Pan, Discovery and evaluation of novel anti-inflammatory derivatives of natural bioactive Curcumin, Drug Des. Dev. Ther. 8 (2014) 2161–2171.
[23] Y. Wang, J. Xiao, H. Zhou, S. Yang, X. Wu, C. Jiang, Y. Zhao, D. Liang, X. Li, G. Liang, A novel monocarbonyl analogue of curcumin, (1E,4E)-1,5-Bis(2,3-dimethoxyphenyl)penta-1,4-dien-3-one, induced cancer cell H460 apoptosis via activation of endoplasmic reticulum stress signaling pathway, J. Med. Chem. 54 (11) (2011) 3768–3778.
[24] W.Q. Chen, P. Zou, Z.W. Zhao, Q.Y. Weng, X. Chen, S.L. Ying, Q.Q. Ye, Z. Wang, J.S. Ji, G. Liang, Selective killing of gastric cancer cells by a small molecule via targeting TrxR1 and ROS-mediated ER stress activation, Oncotarget 7 (13) (2016) 16593–16609.
[25] D. Shetty, Y.J. Kim, H. Shim, J.P. Snyder, Eliminating the heart from the curcumin molecule: Monocarbonyl Curcumin Mimics (MACs), Molecules 20 (1) (2015) 249–292.
[26] Z.E. Pan, C.W. Chen, Y.L. Zhou, F. Xu, Y.Z. Xu, Synthesis and cytotoxic evaluation of monocarbonyl analogs of curcumin as potential anti-tumor agents, Drug Dev. Res. 77 (1) (2016) 43–49.
[27] L. Lin, Q. Shi, A.K. Nyarko, K.F. Bastow, C.-C. Wu, C.-Y. Su, C.C.Y. Shih, K.-H. Lee, Antitumor agents. 250. Design and synthesis of new curcumin analogues as potential anti-prostate cancer agents, J. Med. Chem. 49 (13) (2006) 3963–3972.
[28] C. Luo, Y. Li, B. Zhou, L. Yang, H. Li, Z.H. Feng, Y. Li, J.G. Long, J.K. Liu, A monocarbonyl analogue of Curcumin, 1,5-bis(3-hydroxyphenyl)-1,4-pentadiene-3-one (Ca 37), exhibits potent growth suppressive activity and enhances the inhibitory effect of Curcumin on human prostate cancer cells, Apoptosis 19 (3) (2014) 542–553.

[29] C. Pignanelli, D. Ma, M. Noel, J. Ropat, F. Mansour, C. Curran, S. Pupulin, K. Larocque, J.Z. Wu, G. Liang, Y. Wang, S. Pandey, Selective targeting of cancer cells by oxidative vulnerabilities with novel curcumin analogs, Scient. Rep. 7 (2017).

[30] V. Rajamanickam, H.P. Zhu, C. Feng, X. Chen, H.L. Zheng, X.H. Xu, Q.Q. Zhang, P. Zou, G.D. He, X.X. Dai, X. Yang, Y. Wang, Z.G. Liu, G. Liang, G.L. Guo, Novel allylated monocarbonyl analogs of Curcumin induce mitotic arrest and apoptosis by reactive oxygen species-mediated endoplasmic reticulum stress and inhibition of STAT3, Oncotarget 8 (60) (2017) 101112–101129.

[31] J. Xiao, Y. Wang, J. Peng, L. Guo, J. Hu, M.H. Cao, X. Zhang, H.Q. Zhang, Z.G. Wang, X.K. Li, S.L. Yang, H.L. Yang, G. Liang, A synthetic compound, 1,5-bis(2-methoxyphenyl)penta-1,4-dien-3-one (B63), induces apoptosis and activates endoplasmic reticulum stress in non-small cell lung cancer cells, Int. J. Cancer 131 (6) (2012) 1455–1465.

[32] L.P. Chen, Q. Li, B.X. Weng, J.B. Wang, Y.Y. Zhou, D.Z. Cheng, T. Sirirak, P.H. Qiu, J.Z. Wu, Design, synthesis, anti-lung cancer activity, and chemosensitization of tumor-selective MCACs based on ROS-mediated JNK pathway activation and NF-kappa B pathway inhibition, Eur. J. Med. Chem. 151 (2018) 508–519.

[33] Z.G. Liu, Y.S. Sun, L.Q. Ren, Y. Huang, Y.P. Cai, Q.Y. Weng, X.Q. Shen, X.K. Li, G. Liang, Y. Wang, Evaluation of a Curcumin analog as an anti-cancer agent inducing ER stress-mediated apoptosis in non-small cell lung cancer cells, BMC Cancer 13 (2013).

[34] G. Liang, L. Shao, Y. Wang, C. Zhao, Y. Chu, J. Xiao, Y. Zhao, X. Li, S. Yang, Exploration and synthesis of Curcumin analogues with improved structural stability both in vitro and in vivo as cytotoxic agents, Bioorg. Med. Chem. 17 (6) (2009) 2623–2631.

[35] G. Badr, H.I. Gul, C. Yamali, A.A.M. Mohamed, B.M. Badr, M. Gul, A. Abo Markeb, N. Abo El-Maali, Curcumin analogue 1,5-bis(4-hydroxy-3-((4-methylpiperazin-1-yl) methyl)phenyl)penta-1,4-dien-3-one mediates growth arrest and apoptosis by targeting the PI3K/AKT/mTOR and PKC-theta signaling pathways in human breast carcinoma cells, Bioorg. Chem. 78 (2018) 46–57.

[36] H.S. Ban, H. Nakamura, Boron-based drug design, Chem. Rec. 15 (3) (2015) 616–635.

[37] M. Scholz, E. Hey-Hawkins, Carbaboranes as pharmacophores: properties, synthesis, and application strategies, Chem. Rev. 111 (11) (2011) 7035–7062.

[38] F. Issa, M. Kassiou, L.M. Rendina, Boron in drug discovery: carboranes as unique pharmacophores in biologically active compounds, Chem. Rev. 111 (9) (2011) 5701–5722.

[39] R.N. Grimes, Carboranes, third ed., Academic Press, 2016.

[40] J.F. Valliant, K.J. Guenther, A.S. King, P. Morel, P. Schaffer, O.O. Sogbein, K.A. Stephenson, The medicinal chemistry of carboranes, Coord. Chem. Rev. 232 (1–2) (2002) 173–230.

[41] K. Watanabe, M. Hirata, T. Tominari, C. Matsumoto, Y. Endo, G. Murphy, H. Nagase, M. Inada, C. Miyaura, BA321, a novel carborane analog that binds to androgen and estrogen receptors, acts as a new selective androgen receptor modulator of bone in male mice, Biochem. Biophys. Res. Commun. 478 (1) (2016) 279–285.

[42] M.E. El-Zaria, A.R. Genady, N. Janzen, C.I. Petlura, D.R.B. Vera, J.F. Valliant, Preparation and evaluation of carborane-derived inhibitors of prostate specific membrane antigen (PSMA), Dalton Trans. 43 (13) (2014) 4950–4961.

[43] K. Ohta, T. Iijima, E. Kawachi, H. Kagechika, Y. Endo, Novel retinoid X receptor (RXR) antagonists having a dicarba-closo-dodecaborane as a hydrophobic moiety, Bioorg. Med. Chem. Lett. 14 (23) (2004) 5913–5918.

[44] P. Cígler, M. Kožíšek, P. Řezáčová, J. Brynda, Z. Otwinowski, J. Pokorná, J. Plešek, B. Grüner, L. Dolečková-Marešová, M. Máša, J. Sedláček, J. Bodem, H.-G. Kräusslich, V. Král, J. Konvalinka, From nonpeptide toward noncarbon protease inhibitors: metallacarboranes as specific and potent inhibitors of HIV protease, PNAS 102 (43) (2005) 15394–15399.

[45] I. Fuentes, T. García-Mendiola, S. Sato, M. Pita, H. Nakamura, E. Lorenzo, F. Teixidor, F. Marques, C. Viñas, Metallacarboranes on the road to anticancer therapies: cellular uptake, DNA interaction, and biological evaluation of cobalta-bisdicarbollide [COSAN] − , Chem. Eur. J. 24 (65) (2018) 17239–17254.

[46] D. Gabel, Safety and efficacy in boron neutron capture therapy, in: D. Gabel, R. Moss (Eds.), Boron Neutron Capture Therapy: Toward Clinical Trials of Glioma Treatment, Springer, US, Boston, MA, 1992, pp. 7–13.

[47] G. Locher, Biological effects and therapeutic possibilities of neutrons, Am. J. Roentgenol. 36 (1936) 1–13.

[48] T. Pinelli, A. Zonta, S. Altieri, S. Barni, A. Braghieri, P. Pedroni, P. Bruschi, P. Chiari, C. Ferrari, F. Fossati, R. Nano, S.N. Tata, U. Prati, G. Ricevuti, L. Roveda, C. Zonta, TAOrMINA: From the first idea to the application to the human liver; 2002.

[49] T. Pinelli, S. Altieri, F. Fossati, A. Zonta, D. Cossard, U. Prati, L. Roveda, G. Ricevuti, R. Nano, Development of a method to use boron neutron capture therapy for diffused tumours of liver (Taormina project); 1996.

[50] R.F. Barth, J.A. Coderre, M.G.H. Vicente, T.E. Blue, Boron neutron capture therapy of cancer: Current status and future prospects, Clin. Canc. Res. 11 (11) (2005) 3987–4002.

[51] M.F. Hawthorne, M.W. Lee, A critical assessment of boron target compounds for boron neutron capture therapy, J. NeuroOncol. 62 (1) (2003) 33–45.

[52] R.F. Barth, A critical assessment of boron neutron capture therapy: an overview, J. NeuroOncol. 62 (1) (2003) 1–5.

[53] S. Geninatti-Crich, D. Alberti, I. Szabo, A. Deagostino, A. Toppino, A. Barge, F. Ballarini, S. Bortolussi, P. Bruschi, N. Protti, S. Stella, S. Altieri, P. Venturello, S. Aime, MRI-guided neutron capture therapy by use of a dual gadolinium/boron agent targeted at tumour cells through upregulated low-density lipoprotein transporters, Chem. Eur. J. 17 (30) (2011) 8479–8486.

[54] D. Alberti, A. Toppino, S.G. Crich, C. Meraldi, C. Prandi, N. Protti, S. Bortolussi, S. Altieri, S. Aime, A. Deagostino, Synthesis of a carborane-containing cholesterol derivative and evaluation as a potential dual agent for MRI/BNCT applications, Org. Biomol. Chem. 12 (15) (2014) 2457–2467.

[55] A. Toppino, M.E. Bova, S.G. Crich, D. Alberti, E. Diana, A. Barge, S. Aime, P. Venturello, A. Deagostino, A. Carborane-Derivative, “Click” Reaction under heterogeneous conditions for the synthesis of a promising lipophilic MRI/GdBNCT agent, Chem. Eur. J. 19 (2) (2013) 720–727.

[56] P. Boggio, A. Toppino, S. Geninatti-Crich, D. Alberti, D. Marabello, C. Medana, C. Prandi, P. Venturello, S. Aime, A. Deagostino, Hydroboration reaction as a key for a straightforward synthesis of new MRI-NCT agents org, Biomol. Chem. 13 (11) (2015) 3288–3297.

[57] D. Alberti, N. Protti, A. Toppino, A. Deagostino, S. Lanzardo, S. Bortolussi, S. Altieri, C. Voena, R. Chiarle, S.G. Crich, S. Aime, A theranostic approach based on the use of a dual boron/Gd agent to improve the efficacy of Boron Neutron Capture Therapy in the lung cancer treatment, Nanomedicine 11 (2015) 741–750.

[58] D. Alberti, A. Deagostino, A. Toppino, N. Protti, S. Bortolussi, S. Altieri, S. Aime, S. Geninatti Crich, An innovative therapeutic approach for malignant mesothelioma treatment based on the use of Gd/boron multimodal probes for MRI guided BNCT, J. Contr. Rel. 280 (2018) 31–38.

[59] D. Alberti, N. Protti, M. Franck, R. Stefania, S. Bortolussi, S. Altieri, A. Deagostino, S. Aime, S.G. Crich, Theranostic nanoparticles loaded with imaging probes and rubrocurcumin for combined cancer therapy by folate receptor targeting, Chemmedchem 12 (7) (2017) 502–509.

[60] H.B. Woo, W.-S. Shin, S. Lee, C.M. Ahn, Synthesis of novel Curcumin mimics with asymmetrical units and their anti-angiogenic activity, Bioorg. Med. Chem. Lett. 15 (16) (2005) 3782–3786.

[61] P. Anand, S.G. Thomas, A.B. Kunnumakkara, C. Sundaram, K.B. Harikumar, B. Sung, S.T. Tharakan, K. Misra, I.K. Priyadarsini, K.N. Rajasekharan, B.B. Aggarwal, Biological activities of Curcumin and its analogues (Congeners) made by man and Mother Nature, Biochem. Pharmacol. 76 (11) (2008) 1590–1611.

[62] Y. Porat, A. Abramowitz, E. Gazit, Inhibition of amyloid fibril formation by polyphenols: structural similarity and aromatic interactions as a common inhibition mechanism, Chem. Biol. Drug Design 67 (1) (2006) 27–37.

[63] A.A. Reinke, J.E. Gestwicki, Structure–activity relationships of amyloid beta-aggregation inhibitors based on curcumin: influence of linker length and flexibility, Chem. Biol. Drug Design 70 (3) (2007) 206–215.

[64] P. Dozzo, R.A. Kasar, S.B. Kahl, Simple, High-Yield Methods for the Synthesis of Aldehydes Directly from o-, m-, and p-Carborane and Their Further Conversions, Inorg. Chem. 44 (22) (2005) 8053–8057.

[65] P.-C. Leow, P. Bahety, C.P. Boon, C.Y. Lee, K.L. Tan, T. Yang, P.-L.R. Ee, Functionalized Curcumin analogs as potent modulators of the Wnt/β-catenin signaling pathway, Eur. J. Med. Chem. 71 (2014) 67–80.

[66] M. Markert, R. Mahrwald, LiClO4-Amine mediated direct aldol process, Synthesis 2004 (09) (2004) 1429–1433.

[67] A. Arnold, M. Markert, R. Mahrwald, Amine-catalyzed aldol condensation in the presence of lithium perchlorate, Synthesis 2006 (07) (2006) 1099–1102.

[68] J. van Meerloo, G.J.L. Kaspers, J. Cloos, Cancer Cell Culture -Methods and Protocols, Humana Press, 2011.

[69] J.A. Quincoces Suarez, D.G. Rando, R.P. Santos, C.P. Gonçalves, E. Ferreira, J.E. de Carvalho, L. Kohn, D.A. Maria, F. Faião-Flores, D. Michalik, M.C. Marcucci, C. Vogel, New antitumoral agents I: In vitro anticancer activity and in vivo acute toxicity of synthetic 1,5-bis(4-hydroxy-3-methoxyphenyl)-1,4-pentadien-3-one and derivatives, Bioorg. Med. Chem. 18(17) (2010) 6275-6281.

[70] H. LeVine, [18] Quantification of β-sheet amyloid fibril structures with thioflavin T, Method. Enzymol. Academic Press, 1999, pp. 274–284.

[71] K.-N. Liu, C.-M. Lai, Y.-T. Lee, S.-N. Wang, R.P.Y. Chen, J.-S. Jan, H.-S. Liu, S.S.S. Wang, Curcumin's pre-incubation temperature affects its inhibitory potency toward amyloid fibrillation and fibril-induced cytotoxicity of lysozyme, Biochim. Biophys. Acta 1820 (11) (2012) 1774–1786.

[72] S.S.S. Wang, K.-N. Liu, W.-H. Lee, Effect of Curcumin on the amyloid fibrillogenesis of hen egg-white lysozyme, Biophys. Chem. 144 (1) (2009) 78–87.

[73] P. Patel, K. Parmar, D. Patel, S. Kumar, M. Trivedi, M. Das, Inhibition of amyloid fibril formation of lysozyme by ascorbic acid and a probable mechanism of action, Int. J. Biol. Macromol. 114 (2018) 666–678.

[74] S.K. Maji, M.H. Perrin, M.R. Sawaya, S. Jessberger, K. Vadodaria, R.A. Rissman, P.S. Singru, K.P.R. Nilsson, R. Simon, D. Schubert, D. Eisenberg, J. Rivier, P. Sawchenko, W. Vale, R. Riek, Functional amyloids as natural storage of peptide hormones in pituitary secretory granules, Science 325 (5938) (2009) 328–332.

[75] P.K. Singh, V. Kotia, D. Ghosh, G.M. Mohite, A. Kumar, S.K. Maji, Curcumin modulates α-synuclein aggregation and toxicity, ACS Chem. Neurosci. 4 (3) (2013) 393–407.

[76] M. Miyashita, A. Yoshikoshi, P.A. Grieco, Pyridinium p-toluenesulfonate. A mild and efficient catalyst for the tetrahydropyranylation of alcohols, J. Org. Chem. 42 (23) (1977) 3772–3774.

[77] S. Ying, X. Du, W. Fu, D. Yun, L. Chen, Y. Cai, Q. Xu, J. Wu, W. Li, G. Liang, Synthesis, biological evaluation, QSAR and molecular dynamics simulation studies of potential fibroblast growth factor receptor 1 inhibitors for the treatment of gastric cancer, Eur. J. Med. Chem. 127 (2017) 885–899.